Differences in reactivity of oxide growth during the oxidation of Zircaloy-4 in water vapour before and after the kinetic transition

Marc Tupin, Michèle Pijolat, Françoise Valdivieso, Michel Soustelle, A. Frichet, P. Barberis

J. Nuclear Materials, 003, 117(2-3), 130-44, doi:10.1016/S0022-3115(02)01704-X

Differences in reactivity of oxide growth during the oxidation of Zircaloy-4 in water vapour before and after the kinetic transition

M. TUPIN[A,C], M. PIJOLAT [A](*), F. VALDIVIESO[A], M. SOUSTELLE[A], A. FRICHET[C], P. BARBERIS[B]

[A] *Laboratoire des Procédés en Milieux Granulaires CNRS UMR 5148, Centre SPIN, Ecole Nationale Supérieure des Mines,158 Cours Fauriel, 42023 Saint-Etienne Cedex 2, France*
[B] *Cézus, Centre de Recherche, 73403 Ugine Cédex, France*
[C] *Framatome ANP, Direction Conception et Ventes, 10 rue J. Recamier, 69456 Lyon, Cédex 06 France*

(*) *mpijolat@emse.fr*

Key words:

Zircaloy-4 ; oxidation ; kinetics ; water vapour ; steady state ; rate-limiting-step.

Abstract

The oxidation of Zircaloy-4 by water vapour has been studied between 500 and 550 °C, the water vapour partial pressure ranging in 13–80 hPa, using isothermal and isobaric thermogravimetry, and calorimetry. During gravimetry experiments, sudden changes in temperature or water vapour pressure have also been performed. It results that the approximations of steady state and rate-limiting step are only valid before the kinetic transition. In the post-transition region, a significant influence of water vapour and hydrogen partial pressures has been found, contrarily to the kinetic behaviour before the transition (which is in this last case, in good agreement with a rate-limiting step of diffusion of oxygen vacancies). It comes out that the post-transition kinetic behaviour is definitely not the same as before the transition.

Subject-index terms:

C0500; C0800; K0100; Z0100

1. Introduction

Despite an abundant literature on the oxidation kinetics of Zircaloy-4 by water vapour or oxygen, the mechanisms and the rate-controlling step of the formation of zirconia are not yet very clearly established. However, some important features can be drawn from the various articles devoted to the interpretation of the kinetic behaviour of Zircaloy-4:

- • there exists a kinetic transition whatever the oxidant is (oxygen, water vapour or liquid water),
- • the oxidation kinetics during the pre-transition period is not parabolic and follows approximately the cubic law [1, 2 and 3],
- • the transition, which corresponds to an increase of the rate, is associated with the apparition of cracks and pores in the oxide layer [2, 4 and 22],
- • the post-transition oxidation curves have been found to be linear or resulting from cyclic periods of increasing and decreasing rate.

1.1. Pre-transition

Several explanations have been proposed to account for the non-parabolic oxidation rate in the pre-transition region: oxygen diffusion along grain boundaries of the oxide layer in which the grain size [5 and 6] or the compressive stresses [7] vary with increasing thickness, effect of an electric field on the diffusion of charged species [8], ...

However, it must be recognised that this question is still a mater of debate, probably because in many attempts, the experimental results were approximately well fitted by the expression of the different kinetic rate laws used by the authors. But it can generally be noticed that the accuracy is not sufficient enough to make the result absolutely unambiguous due to various reasons like the number of experimental points, the error on the measurements, the use of logarithmic scales ...
Moreover, it remains some kinetic laws that have, to our knowledge, never been tested in the case of Zircaloy-4 oxidation, as those proposed by Evans [9 and 10] or Smeltzer [11] when the diffusing species encounter 'abnormal' energy barriers in the oxide lattice like cracks or short circuits, respectively.
The variations of the oxidation rate of Zircaloy with temperature and pressure have been investigated. Due to the diversity in the materials, the experimental conditions and the expressions of the rate used by the authors, the values of the (apparent) activation energy are spread in the range 120–172 kJ mol^{-1} with oxygen.
The influence of oxygen pressure has been studied by several authors [2, 3 and 12] who found that the rate was independent of the pressure in the pre-transition period. This is in agreement with a rate-limiting step of diffusion of oxygen vacancies in the oxide layer.
When the oxidation is performed with water vapour, the results are controversial: Dawson et al. [2] and Cox [12] did not find any influence with Zircaloy-2 at 450 °C whereas a significant increase in the oxidation rate was observed with increasing water vapour pressure in other works [13, 14].

1.2. Transition

The origin of the kinetic transition has been attributed to the formation of a porous layer with partial loss of its protective character due to the development of cracks penetrating close to the metal/oxide interface [2 and 4]. It was proposed also that the transition could be due to a stress relaxation associated to the quadratic to monoclinic transformation, however this has recently been discarded [15 and 16].
The position of the kinetic transition can be determined by the oxide layer thickness at which occurs the minimum of the rate [2]. It varies with many factors like temperature, pressure, precipitates, ... A significant influence of pressure has been found with both oxygen and water vapour: the higher the pressure, the higher the thickness at the transition [2].

1.3. Post-transition

In the post-transition period, the quasi-linear curves have been interpreted as the result of at least three possible processes:

- • a succession of approximately parabolic periods [17],
- • a rate-controlling diffusion in a dense layer of constant thickness close to the metal/oxide interface,
- • with oxygen, the direct contact between the gas and the metal (no barrier layer) [12].

The study of the influence of oxygen or water vapour pressure is in favour of the last proposal since several authors have observed an increase in the oxidation rate with a pressure increase [2, 12 and 13]. By doing a series of oxygen pressure changes during an experiment, Cox [12] put in evidence that the pressure dependence of the rate measured just after the change was linear. But after an equilibration time, the value of the oxidation rate became nearly the same as before the pressure change. These results were attributed to the gas transport through the pores of the oxide layer.
In recent works [18, 19 and 20], we have done similar experiments, by changing suddenly the temperature or the pressure of one of the reacting gases to obtain the ratio of the rates just after and before the change. This method was applied in order to determine experimentally

the variations of the so-called 'growth reactivity' as a function of temperature and gas pressure according to the following general expression of the rate (1):

$$\frac{d\xi}{dt} = n_0 \ \phi(T,P,\ldots)\ E(t) \qquad (1)$$

where ξ is the extent of reaction (in mol), n_0 is the initial number of moles, ϕ is the surfacic reactivity of growth (in mol s^{-1} m^{-2}), and $E(t)$ (in m^2 mol^{-1}) is representative of the dimensions of the reaction area where the rate-controlling step is located.
For example in the case of the parabolic law expected for a diffusion control in an oxidised platelet with initial thickness X_0 and surface S_0:

$$\phi(T,P,\ldots) = \frac{D\Delta C}{X_0} \qquad \text{(in mol.m}^{-2}\text{.s}^{-1}\text{)} \qquad (2)$$

$$E(t) = \frac{2S_0X_0}{n_0}\frac{1}{X} \qquad \text{(in m}^2\text{.mol}^{-1}\text{)} \qquad (3)$$

where D is the coefficient of diffusion, and ΔC the difference in concentrations of the diffusing species at the two interfaces.
The separation between the time t and physico-chemical parameters (P,T,...) has already been suggested [21], in a particular case of Eq. (1). The interest of the general Eq. (1) is that it does not preclude any hypothesis on the mechanism excepted two fundamental approximations:

(i) the steady state,

(ii) the rate-limiting step of zirconia growth.

Some remarks must be pointed out concerning the use of Eq. (1):

- in some particular cases, where two limiting steps with similar rates occur in the same reaction zone, Eq. (1) may also be obtained,
- in other few cases where the rate-limiting step is the diffusion of charged species in an electric field, Eq. (1) cannot be obtained.

In the following, we will only consider cases in which the approximation of the rate-limiting step leads to Eq. (1).
In the oxidation of metals or alloys the establishment of a steady state can be achieved when there is no accumulation of the intermediates of reaction at the interfaces or in the oxide layer, and also if the size of the reaction areas does not change very quickly during the reaction [18]. As far as we know, there has never been any attempt to test the validity of the approximation of the steady state in the oxidation of Zircaloy-4. It is possible to make the appropriate experiment using a simultaneous gravimetric and calorimetric analysis [18, 19 and 20]. It is effectively easy to show that the condition of the steady state implies that the rates obtained by two different methods should remain proportional during all the reaction.
The approximation of the rate-limiting step can be validated by experiments based on a sudden change in temperature (or pressure). This method has already been successfully used in our previous studies on various reaction systems [18, 19 and 20] since it provides the domain of the extent of reaction in which it is possible to use Eq. (1) and its consequences.
Due to the lack of consistent data on the effect of the water vapour pressure on the rate variations before and after the transition, and in order to verify the validity of the assumptions generally used to account for the experimental results, it was thus decided to follow the oxidation kinetics of Zircaloy-4 around 500 °C and in water vapour in order to answer the following questions:

1. Does the oxidation proceeds in a steady state in the pre- and post-transition domains?

2. Is the approximation of a rate-controlling step valid in one of these domains (or both)?

3. In case of a rate-controlling step found in one domain, how are the variations of the reactivity of growth (ϕ) as a function of water vapour pressure?

The main objective of this article is to clearly put in evidence the differences between the pre- and the post-transition from a kinetic point of view, and to quantify them in order to propose reliable mechanisms.

2. Experimental

Specimens from a standard 0.41 mm sheet of recrystallized Zircaloy-4 provided by Cezus were cut to 10 mm × 10 mm for gravimetric experiments and to 5 mm × 15 mm for simultaneous gravimetric–calorimetric experiments. The alloy composition is indicated in Table I. The samples surface was simply cleaned first with an equimolar solution of ethanol and acetone in ultrasonic waves, then with pure ethanol and dried in compressed air.
The oxidation kinetics in water vapour–hydrogen mixture in helium (flow rate: 2.3 l h^{-1}) was followed by means of a symmetrical microbalance (Setaram TAG 16) equipped with a thermoregulated cooling fluid and two humidity sensors (TRANSMICOR 241-242 CORECI) placed just before and after the furnace. The desired partial pressures were obtained using mass flowmeters (Brooks 5850S). The hydrogen pressure was generally fixed at 10 hPa while water vapour pressure was in the range 13–80 hPa. The hydrogen pressure value was chosen in order to make negligible the production of hydrogen by the reaction, taking into account the maximum of rate and the gas flowrate. The water vapour partial pressure in the helium flow was maintained at the appropriate value using thermoregulated water baths.
The simultaneous thermogravimetric–calorimetric experiments were performed with a TG-DSC 111 from Setaram, equipped with a microbalance similar to the TAG 16, and a heat flow sensor type calorimetric device (limit of detection 10 μW).
During some experiments, sudden changes in the hydrogen partial pressure (P_{H_2}) were achieved by modifying the flowmeter setpoint to the desired value, whereas with water vapour (P_{H_2O}) they were done by switching the helium flow from one bath to the other. Sudden changes in temperature (T) were done by means of the regulation system of the furnace. The time necessary to obtain a constant value after the change was 5 min for T and P_{H_2}, and 15 min for P_{H_2O}. In all these experiments (except mentioned) the temperature was fixed to 530 °C after an initial rise from room temperature at a rate of 30 °C min^{-1}.
Several techniques were used to characterise the oxidised samples:

- The pore structure of the oxide layer at various stages of the oxidation was observed by scanning electron microscopy (SEM, DSM960A, Zeiss).
- The concentration profiles in the oxidised samples were obtained by glow discharge spectroscopy (GDS) using a Jobin-Yvon JY50 for the pre-transition and a LECO GDS 750 A for the post-transition.
- The hydrogen pick-up has been measured by CEZUS, using hot-extraction under argon (Strohlein 2500). The amount in hydrogen absorbed after the transition is obtained by subtracting to the measured value the amount absorbed up to the transition.

3. Results

3.1. Steady state approximation

A kinetic curve (mass gain versus time) and its derivative $\left(\frac{dm}{dt}\right)$ obtained at 530 °C in a mixture of water vapour (13 hPa) and hydrogen (10 hPa) are represented on Fig. 1, which shows clearly the transition.

Fig. 2(a) gives the variations of the rate of weight increase $\left(\frac{dm}{dt}\right)$ and of the heat flow (DH) as a function of time in the pre-transition region (at 550 °C). A scaling factor allowing to superimpose the rate curves could be found, as it can be seen in the figure.

Fig. 2(b) represents $\mathrm{d}m/\mathrm{d}t$ for another experiment performed in the same conditions, showing both the pre- and post-transition regions. It appears that a single scaling factor could not be found to superimpose the two curves $\mathrm{d}m/\mathrm{d}t$ and DH versus time. The rates measured by the two methods (gravimetry, calorimetry) being proportional in the pre-transition period, the steady state approximation is valid without any doubt. After the transition, the two curves can be more or less superimposed (Fig. 2(c)), but the scaling factor leading to the best agreement is different from the one obtained before the transition. Thus, the steady state might be assumed in the post-transition period, but the change in the scaling factor remains unexplained.

Consequently the relationship (4) between the mass gain (Δm, (g)) and the thickness of the oxide layer (X) is, during the pre-transition period:

$$X = \frac{1}{2S_0}\frac{M_{ZrO_2}}{\rho_{ZrO_2}}\frac{\Delta m}{M_{O_2}} \qquad (4)$$

where ρ_{ZrO_2} is the mass density of zirconia (6 g cm^{-3} for the tetragonal phase), M_{ZrO2} and M_{O2} the molar masses of zirconia and oxygen (g mol^{-1}), S_0 the surface of the sample (cm^2).

After the kinetic transition, the use of Eq. (4) gives a thickness, which would be an 'equivalent' one if the steady state assumption is not valid.

3.2. Rate-limiting step approximation

When the rate-limiting step approximation can be used, the rate of reaction is given by that of one of the steps of the mechanism (elementary reactions like adsorption or interfacial reaction, and diffusion steps) and consequently the steady state is established. Eq. (1) can then be used to express the variation of the rate with the intensive variables (temperature, pressure, ...) and the time. In isothermal and isobaric conditions, the variation of the rate with the time of reaction is given by $E(t)$ while ϕ (T,P,...) remains constant. A sudden change in T or P during an experiment will thus induce a change in ϕ only, while $E(t)$ will remain approximately the same before and after the change. It comes out that the ratio of the rate measured on the right side of the change to the rate measured on the left side is simply equal to the ratio of $\frac{\phi_r}{\phi_l}$ according to Eq. (1). So by doing a series of sudden changes at different times of reaction, the ratio of the rates will be constant as long as Eq. (1), or the approximation of the rate-limiting step, applies. The result of this method, that we have called the 'ϕE test', is represented on Fig. 3(a) and (b), in case of a sudden change in temperature from 530 to 500 °C (P_{H_2O} =13 hPa, P_{H_2} =10 hPa).

Considering the experimental error bars, the ratio keeps a constant value (2.32 ± 3%) during the pre-transition domain up to 3 μm (Fig. 3(a)). Then it decreases (1.9 at 3.5 μm) and takes

lower values which remain between 1.16 and 1.38 during the post-transition domain (Fig. 3(b)), but the error bars do not overlap. Thus it can be stated that:

- the ϕE test is validated in the pre-transition domain,
- the kinetic transition occurs before the minimum of the rate in weight increase, which is 3 µm instead of 4 µm in the described experiment,
- the ϕE test is not verified in the post-transition domain since the ratio of the rates is not constant with the extent of weight increase, therefore the rate-limiting step approximation is not valid.

3.3. Influence of H_2O and H_2 partial pressure

3.3.1- Pre-transition:

When a sudden change in water vapour or hydrogen pressure (from P_0 to P) is performed at a given thickness X, the ratio of the rates just after and before the change is equal to (from Eq. (1)): $\frac{\Phi(P)}{\Phi(P_0)}$). Thus, the variations of ϕ with the gas partial pressure P are easily obtained. The experiments have been done at 500 °C, with 10 hPa in hydrogen and a water vapour pressure varying from 13 hPa (initially) up to 80 hPa after the sudden change, and 13 hPa in water vapour and a hydrogen pressure varying from 10 hPa (initially) up to 40 hPa after the sudden change.

The values obtained for the ratios $\frac{\Phi(P)}{\Phi(P_0)}$ are given in Table II for both series. They show that there is no influence of P_{H_2O} nor P_{H_2} on the reactivity of growth during the pre-transition.

3.3.2- Post-transition/influence of water vapour partial pressure

The curves obtained in isothermal (530 °C) and isobaric conditions are shown in Fig. 4, which represents the weight increase and the rate $\frac{dm}{dt}$ versus time, for 13 and 73 hPa in water vapour.

It is observed that when H_2O partial pressure has been fixed to 73 hPa, the rate increase occurs earlier than with 13 hPa and that the average value of the rate of weight increase is higher after the transition.

The results obtained with sudden changes of P_{H_2O} during the post-transition at 530 °C (10 hPa in hydrogen) are given in Table III. A first series of experiments was done changing P_{H_2O} from 13 to 33 hPa at various times of oxidation, examples are shown in Fig. 5. These times correspond to the increasing part of the rate of weight gain just after the kinetic transition (equivalent thickness equal to 6.5 µm), to the first maximum of the rate (11.7 µm), and to the decreasing part after the first maximum (14.5 µm), as indicated in Fig. 1. The values of the ratios in Table III are found to be dependent on the time of oxidation which confirms that the ϕE test is not valid. (This result has already been found using temperature changes in Section 3.2.).

The influence of P_{H_2O} on the rate of weight increase has been followed by making sudden changes in the range 13–73 hPa at the three values of weight increase previously indicated. The values of $\frac{\mathrm{dm}}{\mathrm{dt}}(\mathrm{P})/\frac{\mathrm{dm}}{\mathrm{dt}}(13\ \mathrm{hPa})$ represented as a function of P_{H_2O} in Fig. 6 clearly show the accelerating effect of water vapour pressure on the rate of weight increase.

3.3.3- Post-transition/influence of hydrogen partial pressure

Two experiments of hydrogen partial pressure sudden change have been done at 530 °C from 10 to 40 hPa, and from 10 to 2.5 hPa, starting with 13 hPa in P_{H_2O}. The results, given in Table IV, indicate that contrarily to the pre-transition domain, the hydrogen partial pressure has an effect on the weight increase. The higher the hydrogen partial pressure, the higher the rate.

3.3.4- Summary

The results obtained in the 3.1, 3.2 and 3.3 have been summarised in Table V. It results that the kinetic behaviour of the alloy before and after the transition is completely different from the point of view of the steady state approximation, the rate-limiting step of the growth process and the sensitivity to the gaseous atmosphere. This means that the kinetic description in terms of elementary steps of ZrO_2 formation should include these differences: if the rate in the pre-transition can be accounted for by a diffusion of oxygen vacancies as the rate-limiting step, this is no more valid after the transition.

3.4.Characterisation of the samples

To be as realistic as possible, such models must be based on the characterisation of the samples used in this study at various states of oxidation.

3.4.1- SEM

The cross-sectional views of the oxide scale grown during the pre-transition region present a continuous and uniform layer adherent to the substrate. Fig. 7(a) and (b) show micrographs obtained with the same sample oxidised after 4 h at 530 °C in 13 and 10 hPa of water vapour and hydrogen, respectively. The layer thickness calculated from the weight gain is 1.7 μm. No cracks connected to the gaseous atmosphere could be observed; the interface is more or less regularly undulated. Short cracks parallel to the interface appear regularly inside the layer (Fig. 7(b)).

Similar cracks are observed in the samples obtained after a longer oxidation time, i.e. after the kinetic transition. Fig. 8(a) and (b) present typical cross-sectional views. In contrast to the oxide films grown during the pre-transition region, these observations reveal the presence of important cracks perpendicular to the interface and connected to the gaseous atmosphere. Moreover, these perpendicular cracks appear to be connected to parallel cracks probably formed by the coalescence of the initial short ones. These parallel cracks are located at various depths under the surface, as for example 3.5 μm (Fig. 8(a) and (b)) and 30 μm (Fig. 9(a) and (b)). In the samples observed after a sudden change in the water vapour partial pressure (with increasing pressure), the oxide layer (20 μm) is considerably damaged with large and numerous cracks directly connected with the gaseous atmosphere (Fig. 10(a)–(c)).

3.4.2. Glow discharge spectroscopy

This technique has been used to obtain qualitatively the distribution profiles in the elements H, O, Zr, Fe, Cr and Sn contained in three samples oxidised in various conditions:

- at 500 °C (P_{H_2O} =67 hPa, P_{H_2} =27 hPa) and in the pre-transition region (Fig. 11(a)) with an oxide thickness equal to 3 μm (for this sample, the GDS device which has been used did not allowed to record the Zr profile),
- at 530 °C (P_{H_2O} =13 hPa, P_{H_2} =10 hPa) and in the post-transition region (Fig. 11(b)) with an equivalent oxide thickness equal to 11 μm,
- at 530 °C (P_{H_2O} =13 hPa, P_{H_2} =10 hPa) and in the post-transition region (Fig. 11(c)), with an equivalent thickness equal to 11 μm after a sudden change of water vapour pressure from 13 to 40 hPa.

It can be seen that the profile in hydrogen is very different in the pre- and post-transition regions since a peak whose the maximum is located at the oxide/metal interface is present

only in the samples oxidised after the transition. The comparison of zirconium and hydrogen profiles suggests that hydrogen could be concentrated at the interface in the oxide. Nevertheless, the metal/oxide interface being quite undulated, this maximum could also been related to zirconium hydrides in the metallic substrate (see Section 3.4.3). Complementary experiments with an other method such as SIMS could be useful to rule out potential artefacts.

3.4.3- Hydrogen pick-up ratio

The concentration of hydrogen absorbed in the metal, C_H, measured for various samples in pre- and post-transition domains, is indicated in the second column of Table VI. The hydrogen pick-up ratio F represents the amount of hydrogen absorbed in the metal, divided by the amount of gaseous hydrogen which should have been evolved theoretically (considering the weight gain). This ratio F is defined by Eq. (5):

$$F(\%) = \frac{\left(\frac{m_0}{M_{Zr}} - \frac{\Delta m}{2M_0}\right) M_{Zr} \frac{(C_H - C_{Hini})}{10^6}}{2M_H \frac{\left[\Delta m - \left(\frac{m_0}{M_{Zr}} - \frac{\Delta m}{2M_0}\right) M_{Zr} \frac{(C_H - C_{Hini})}{10^6}\right]}{M_0}} \qquad (5)$$

where m_0 is the sample mass (g), C_{Hini} and C_H are the hydrogen concentrations in the starting and oxidised sample respectively (ppm), Δm is the weight gain (g), M_O, M_H, M_{Zr} the molar masses of oxygen, hydrogen and zirconium respectively (g mol^{-1}).
The hydrogen pick-up ratio (%F) is given in the third column of Table VI, the ratio corresponding to the post-transition domain being indicated in the last column (F_{post}). Before the kinetic transition, the metal absorbs a very low amount of hydrogen (much less than 100 ppm), and the H pick-up ratio is around 10%. Beyond the transition, the hydrogen pick-up ratio increases and reaches a constant value between 50% and 60%.
The solubility of hydrogen in Zircaloy-4 being about 500 ppm at 530 °C [22], precipitation of hydrides in the metal probably occurs after the transition.

4. Discussion

4.1. Pre-transition

Since the approximations of steady state and rate-limiting step are valid in the pre-transition region, it is possible to propose (as usually done [5 and 11]) that the growth of zirconia is controlled by the diffusion of oxygen vacancies in the oxide layer. To account for the deviation to the parabolic law (Wagner's model), we have successfully tested the following equation:

$$\frac{dX}{dt} = \frac{k_1}{X} \exp\left(-k_2 X\right) \qquad (6)$$

k_1 and k_2 are constants which significance depends on the physical modelling [8, 9 and 10], as detailed in the following.
The comparison of the numerical fits obtained with various laws (parabolic law, power law, cubic law) is shown in Fig. 12. Eq. (6) leads to a good agreement with the experimental curve. We obtained the same results with all our experimental curves. It can be noticed that the fits with the power and the cubic laws are also good, but there does not exist any modelling to account for these laws and give them a physical meaning.
To our knowledge, two distinct assumptions may lead to the same mathematical law as that given in Eq. (6): firstly the existence of barriers for the diffusing species (pores or cracks distributed at random inside the oxide layer) as proposed earlier by Evans [9] then demonstrated by Cournil and Thomas [10], and secondly the effect of a gradient of compressive stresses in the oxide layer [8]. Concerning the existence of barriers in the oxide

layer, Bossis et al. [23] has recently suggested that the cracks present in oxide scales grown in high water vapour pressure were probably obstacles for the diffusing species.
The observations we have done on cross-sectional micrographs are in favour of the first assumption since numerous short cracks are present in the oxide scale; moreover the coefficient k_2 of Eq. (6), which would in that case represent the number, per length unit, of barriers which cannot be passed through by the diffusing species, takes a value (from the numerical fitting) which is close to 1 μm^{-1}. This value is acceptable with respect to the SEM observations (cf. Fig. 7).
The use of Eq. (6) as the rate law in the pre-transition region gives for the reactivity of growth (ϕ) and the E function the following expressions:

$$\phi = \frac{D_V \Delta C_V}{X_0} \ (\text{mol.m}^{-2}.\text{s}^{-1}) \qquad (7)$$

$$E(t) = \frac{2 S_0 X_0}{n_0} \frac{\exp(-k_2 X)}{X} \ (\text{m}^2.\text{mol}^{-1}) \qquad (8)$$

where D_V is the diffusion coefficient of oxygen vacancies, ΔC_V is the difference of concentrations in oxygen vacancies between the two interfaces, and X_0 is a characteristic length like the thickness of the initial sample (in that case, $k_1 = V_{ox} D_V \Delta C_V$ where V_{ox} is the molar volume of the oxide). It is useful to recall that Eqs. ((6), (7) and (8)) are obtained if factors such as electric fields, effect of the alloying elements, ... can be neglected. This is not obviously the case for different alloy compositions or oxidation conditions.
It can be outlined that the expression of the rate from Eqs. ((6) and (7)) is compatible with the validity of the φE test by sudden changes of temperature provided that k_2 is constant with the thickness X and with the temperature.
Comparing this rate law with the diffusion rate law in the absence of barriers (Wagner's model, cf. Eqs ((2) and (3))), it can be noticed that the reactivity of growth φ takes the same expression in both cases. The difference lies in the expression of the function E: for a given thickness X, E is smaller in this model than in Wagner's model (Eq. (3)) due to the term $\exp(-k_2 X)$.
A simple mechanism of growth of ZrO_2 can be written with the following elementary steps, if we suppose neutral oxygen vacancies:

(1) adsorption step on a surface site noted '*s*':

$H_2O + s \rightleftarrows H_2O - s$

(2) external interface reaction step:

$H_2O - s + V_{O_{ext}} \rightleftarrows H_2 - s + O_{O_{ext}}^{\chi}$

(3) hydrogen desorption step:

$H_2 - s \rightleftarrows H_2 + s$

(4) oxygen vacancies diffusion:

$V_{O_{int}}^{\chi} \rightarrow V_{O_{ext}}^{\chi}$ and $O_{O_{ext}}^{\chi} \rightarrow O_{O_{int}}^{\chi}$

(5) internal interface reaction step:

$$Zr_{(métal)} \underset{\rightarrow}{\leftarrow} Zr_{Zr}^{x} + 2V_{O_{int}}^{x}$$

K_i (i=1, 2, 3 or 5) will represent the equilibrium constant of the ith elementary step.

A linear combination of the steps (1)–(5) (2×[(1)+(2)+(3)+(4)]+(5)) leads to the stoichiometric equation:

$$Zr+2H_2O=ZrO_2+2H_2 \quad (9)$$

It is easy to obtain the expression of ϕ from the calculation of the oxygen vacancy concentrations at the two interfaces:

$$\phi = D_V K_5^{1/2}\left(1-\frac{P_{H_2}}{P_{H_2O}K^{1/2}}\right)\approx D_V K_5^{1/2} \quad (10)$$

where K is the equilibrium constant of the reaction of oxidation of zirconium by H_2O. Its value is 1.74×10^{38} at 500 °C, so the term $\frac{P_{H_2}}{P_{H_2O}K^{1/2}}$ can obviously be neglected compared to 1.

This mechanism does not account for the insertion of hydrogen in the metal (which remains very low in pre-transition, see Table VI). It is probable that hydrogen is incorporated via an other pathway such as the diffusion of interstitial hydrogen through the oxide layer.

A similar expression of ϕ (Eq. (10)) can be obtained supposing ionised oxygen vacancies, $V_O^{\cdot}$ or $V_O^{\cdot\cdot}$ (and assuming that the oxide layer is thick, so that the effect of an electric field can be neglected).

However, if ionised vacancies are involved instead of neutral ones, the parallel diffusion of electrons must be assumed in order to respect the electroneutrality of the crystal: several assumptions can then be done to take into account the possible effects of electric fields on the diffusion of these charged species. The analysis of the corresponding various rate laws cannot explain our experimental results with respect to both the shape of the kinetic rate versus time and the result of the ϕE test [24]. This will not be detailed in the present study, since it can be seen that Eq. (10) is in good agreement with the experimental results and particularly with the absence of influence of the partial pressure in water vapour in the pre-transition domain.

Finally, the pre-transition stage can be explained by a rate-limiting step of oxygen diffusion in the oxide layer, the departure from the parabolic law being accounted for by the existence of diffusion barriers in the layer.

4.2. Kinetic transition

It is clear from the results of the sudden change method (cf. Fig. 3) that the rate-limiting step controlling the beginning of the oxidation is no longer valid even before the rate has reached its minimal value. Consequently the thickness at the kinetic transition should preferably be defined by the thickness at which the ratio of the rates measured in the sudden change experiments begins to decrease. The degradation of the oxide layer associated to the perpendicular cracks connected to the gaseous atmosphere is observed on samples oxidised precisely immediately after this point.

It is interesting to note that the previous explanations of the kinetic transition origin (a successive of quasi-parabolic diffusion-controlled periods, or a rate-limiting step of diffusion in a dense layer of constant thickness close to the metal/oxide interface) are in contradiction with our results with respect to the ϕE test. Effectively in both cases, the surfacic reactivity of growth (φ) would remain unchanged, whereas the function E would be eliminated in the ratio of the rates.

The ‘end’ of the kinetic transition can be defined as the point of inflexion which appears in the first increasing period of the rate (at about 7–8 μm in the experiment of Fig. 1). It is just a suggestion we propose here in order to define a post-transition regime.

4.3. Post-transition

In the post-transition domain, the rate of oxidation measured from the weight gain undergoes a series of increasing and decreasing periods, like an oscillation around a mean value which appears to be approximately constant with time.
Obviously, the appearance of perpendicular cracks which leads to the change of the morphology of the oxide layer must be directly related to the acceleration of the weight gain after the kinetic transition. The oscillating behaviour of the rate versus time cannot be explained unless a periodical change of morphology occurs, like the appearance of new parallel cracks connected with the gaseous phase, for example, as far as the thickness layer increases. More observations are needed to progress with this possible interpretation.
The water vapour and hydrogen partial pressures have been found to have an influence on the oxidation rate during the post-transition period. Moreover, the variations of the rate with the water vapour pressure do not remain the same (they depend on the layer thickness). These features cannot be simply the consequence of a change of rate-limiting step since we have seen that this approximation has no real meaning after the kinetic transition (the ϕE test was not verified).
It appears that a new mechanism must be considered taking into account the partial pressure effects and the appearance of a porous layer which contains the cracks perpendicular to the surface. The existence of a porous layer over a dense layer has been put in evidence in such alloys, using impedance spectroscopy methods [25 and 26]. The diffusion of the reacting gas through the porous layer may be involved in the post-transition mechanism by considering either the molecules of water or the surface hydroxyl groups as the diffusing species. It is known that such $OH_O^{\bullet\bullet}$ surface defects can be easily formed at the surface of oxide powders like ZrO_2 via the reaction:

$$H_2O + V_{O_{surf}}^{\bullet\bullet} + O_{O_{surf}}^{x} \underset{\rightarrow}{\leftarrow} 2OH_{O_{surf}}^{\bullet} \qquad (11)$$

Moreover previous works have shown a catalytic effect of water vapour on the rate of zirconia grain growth at high temperature [27]. Consequently, we expect that the higher the water vapour pressure the higher the rate of modification of the porous structure of the oxide layer [28]. We thus may propose that $OH_O^{\bullet\bullet}$ groups formed at the external interface could, for one part, recombine and lead to the desorption of hydrogen, and for the other part diffuse through the porous oxide layer until an intermediate interface between the porous and a dense layer near the oxide/metal interface (Fig. 13(b)).
At this intermediate interface, the reaction between adjacent $OH_O^{\bullet}$ groups would liberate hydrogen species, and oxygen ions would subsequently migrate through the dense layer via oxygen vacancies. Obviously this layer would be thin enough to allow a rapid non-limiting oxygen diffusion and the diffusion of hydrogen inwards the metal.
Such a mechanism is under study for the derivation of theoretical rate laws in order to try to describe the variation of the rate with the partial pressures in water vapour and hydrogen. Fig. 13 summarises the difference between the mechanisms proposed for the pre- and post-transition.
It remains some aspects which have not been taken into account in these descriptions like the quadratic-monoclinic transformation [27 and 28], the influence of inter-metallic precipitates [23], the effect of the alloying elements, ... Of course a rigorous modelling of this oxidation reaction requires to consider both the chemical, geometrical and mechanical aspects, and it presently comes out that the changes in mechanism due to the changes of the reaction zones morphology of the oxide layer after the kinetic transition have to be involved.

5. Conclusions

The oxidation of Zircaloy-4 in a mixture of water vapour and hydrogen at 500–530 °C exhibits strong differences between the pre- and the post-transition regions. In the pre-transition region only, the oxidation proceeds via a steady state, and the rate is controlled by a rate-limiting step, which is most probably the diffusion of oxygen vacancies through the oxide layer.

The kinetic transition occurs before the minimum of the rate, and beyond that point the steady state approximation may be still valid, but no rate-limiting step can be assumed.

In the range 13–80 hPa in water vapour, the oxidation of Zircaloy-4 is insensitive to water vapour and hydrogen pressure changes before the kinetic transition only. These two gases have an accelerating effect in the post-transition region.

These differences can be explained by a change in the mechanism of zirconia growth related to changes in the porous structure of the oxide layer which lead to changes in the reaction areas and reactive species involved in the growth of zirconia.

References

[1] H.A. Porte, J.G. Schnizlein, R.C. Vogel, D.F. Fisher, J.Electrochem. Soc. 107 (1960) 506.
[2] J.K. Dawson, G. Long, W.E. Seddon, J.F. White, J. Nucl.Mater. 25 (1968) 179.
[3] T. Arima, K. Moriyam, N. Gaja, H. Furuya, K. Idemitsu, Y. Inagaki, J. Nucl. Mater. 257 (1998) 67.
[4] B. Cox, J. Nucl. Mater. 148 (1987) 332.
[5] G.P. Sabol, S.B. Dalgoard, J. Electrochem. Soc. 122 (1975) 316.
[6] E.A. Garcia, J. Nucl. Mater. 224 (1995) 299.
[7] C.C. Dollins, M. Jursich, J. Nucl. Mater. 113 (1983) 19.
[8] G.A. Eloff, C.J. Greyling, P.E. Viljoen, J. Nucl. Mater. 199(1993) 285.
[9] U.R. Evans, in: Proceedings of the Ninety-first General Meeting at Louisville, Ky., 12 April 1947, p. 547.
[10] M. Cournil, G. Thomas, J. Chim.-Phys. 74 (1977) 545.
[11] W.W. Smeltzer, R.R. Haering, J.S. Kirkaldy, Acta Metall.19 (1961) 880.
[12] B. Cox, J. Nucl. Mater. 148 (1987) 332.
[13] Y. Ok, Y. Kim, J. Kor. Nucl. Soc. 30 (1998) 396.
[14] B. Cox, Report AECL-4448, 1973.
[15] P. Barberis, J. Nucl. Mater. 226 (1995) 34.
[16] N. Pétigny, P. Barberis, C. Lemaignan, Ch. Valot, M.Lallemant, J. Nucl. Mater. 280 (2000) 318.
[17] M. Parise, thesis, Paris, 1996.
[18] K. Surla, F. Valdivieso, M. Pijolat, M. Soustelle, M. Prin-Lamaze, Ann. Chim. Sci. Mater. 25 (2000) 601.
[19] K. Surla, F. Valdivieso, M. Pijolat, M. Soustelle, M. Prin-Lamaze, Solid State Ionics 143 (2001) 355.
[20] F. Ledoux, F. Valdivieso, M. Pijolat, M. Soustelle, A.Frichet, P. Barberis, Mater. Sci. Forum 369–372 (1) (2001)223.
[21] A. Pacault, C.R. Acad. Sci. Paris 268 (C) (1969) 383.
[22] J.J. Kearns, J. Nucl. Mater. 22 (1967) 292.
[23] P. Bossis, G. Lelievre, P. Barberis, X. Iltis, F. Lefebvre, in:12th International Symposium, ASTM STP1354, West Conshohocken, 2000.
[24] M. Tupin, thesis, Saint-Etienne, 2002.
[25] F. Garzarolli, H. Seidel, R. Tricot, J.P. Gros, in: 9th International Symposium, ASTM STP1132, Philadelphia, 1991.
[26] J.J. Vermoyal, thesis, Grenoble, 2000.
[27] A. Méthivier, thesis, Saint-Etienne, 1992.
[28] X. Guo, Solid State Ionics 112 (1998) 113.

Tables captions

Table I: Composition of the Zircaloy-4 alloy.

C (ppm)	Cr (ppm)	Fe (ppm)	Hf (ppm)	N (ppm)	O_2 (ppm)	Si (ppm)	Sn (%)
106	1075	2203	46	35	1260	35	1.46

Table II: Variation of the reactivity of growth before transition versus partial pressure of water vapour (a) and of hydrogen (b)

(a) Sudden change in partial pressure of water vapour at X = 0.5 µm and for T = 500°C, P_{H_2} = 10 hPa and P_O = 13 hPa		(b) Sudden change in partial pressure of hydrogen at X = 2 µm and for T = 500°C, P_{H_2O} = 13 hPa and P_O = 10 hPa	
P_{H_2O}	$\phi(P_{H_2O})/\phi(P_O)$	P_{H_2}	$\phi(P_{H_2})/\phi(P_O)$
13	1	2	0.94
67	1	10	1
80	1.02	40	0.94

Table III: Variation of the ratio of the rates in post-transition versus partial pressure of water vapour for sudden change at X = 6.5 µm (a), at X = 11.7 µm (b) and at X = 14.5 µm (c) (530°C, P_{H_2} = 10 hPa, P_O = 13 hPa)

(a) X = 6.5 µm		(b) X = 11.7 µm		(c) X = 14.5 µm	
P_{H_2O}	$dm/dt(P_{H_2O})/dm/dt(P_O)$	P_{H_2O}	$dm/dt(P_{H_2O})/dm/dt(P_O)$	P_{H_2O}	$dm/dt(P_{H_2O})/dm/dt(P_O)$
13	1	13	0.94	13	1
19.5	1.3	32	2.12	19.5	1.2
35	2.2	44	2.26	35	1.88
73	4.2	62	3.15	65	2.6
		72	3.2		

Table IV: Variation of the ratio of the rates versus partial pressure of hydrogen for sudden change at X = 6.5 µm (530°C, P_{H_2O} = 13 hPa, P_O = 10 hPa)

P_{H_2}	$dm/dt(P_{H_2})/dm/dt(P_O)$
2	0.86
10	1
40	1.14

Table V: Summary of kinetic results in pre- and post-transition.

	Pre-transition	Post-transition
Steady state	Yes	Probably
ϕE test	Yes	No
Rate-limiting step	Yes	No
Water vapour partial pressure	Insensitive	Accelerating effect (important)
Hydrogen partial pressure	Insensitive	Accelerating effect (small)

Table VI: Hydrogen concentration in the metal (C_H) and total H pick-up ratios for the pre- and post-transition (F_t). The last column presents the H pick-up ratios in post-transition (F_{post}) obtained by subtracting the H absorbed in the pre-transition.

X (µm)	C_H (wt ppm)	F_t (%)	F_{post} (%) post
3	48	11	
5.6	270	33	58
7.4	433	38	57
8.1	617	50	74
11.5	757	47	59
13.8	966	49	59
15.3	969	44	52
21.6	1500	48	54
29.2	2280	53	58

The last column presents the H pick-up ratios in post-transition (F_{post}) obtained by subtracting the H absorbed in the pre-transition.

Figures

Fig. 1: Weight gain (—) and its derivative (---) versus time for Zircaloy-4 at 530°C in water vapour (13 hPa) and hydrogen (10 hPa), showing the pre- and post transition stages.

Fig. 2: Rate of weight gain (--- dm/dt) and heat flow (— DH) versus time for Zircaloy-4 at 550 °C in water vapour (13 hPa) and hydrogen (10 hPa), pre- (a) and post-transition (b), (c) stages.

Fig. 3: Rate of weight gain (550 °C, P_{H2O}=13 hPa, P_{H2}=10 hPa) and ratios of rate before and after the temperature change, in the pre- (a) and post-transition (b) stages.

Fig. 4: Weight gain and its derivative versus time for Zircaloy-4 at 530 °C (10 hPa in hydrogen): 13 hPa (—) and 73 hPa (---) in water vapour.

Fig. 5: Weight increase versus time for Zircaloy-4 at 530 °C (10 hPa in hydrogen) with sudden changes in water vapour partial pressure from 13 to 33 hPa.

Fig. 6: Ratios of weight increase rates before and after the sudden pressure changes at three equivalent thickness: 6.5 µm (♦), 11.7 µm (□) and 14.5 µm (°) (530 °C, 10 hPa in hydrogen).

Fig. 7: Cross-sectional views of the same Zircaloy-4 sample oxidised at 530 °C (thickness ≈2 µm).

Fig. 8: Cross-sectional views of the same Zircaloy-4 sample oxidised at 500 °C (X≈3.5 µm) with different scales for (a) and (b).

Fig.9: Cross-sectional views of the same Zircaloy-4 sample oxidised at 530 °C (X≈30 µm). For (b), an image treatment has been performed to show cracks and pores and the scale is different from that of (a).

Fig. 10: Cross-sectional views of Zircaloy-4 oxidised at 530 °C and submitted to a sudden change of water vapour (from 13 to 73 hPa) (X=20 µm) (a), (b), (c). For (c), an image treatment has been performed to show cracks and pores.

Fig. 11: GDS distribution profiles for the oxidised samples: (a) pre-transition (X≈3 µm), (b) post-transition (X≈11 µm), (c) post-transition sample submitted to a sudden change of water vapour (13 to 40 hPa).

Fig. 12: Rate of oxidation of Zircaloy-4 as a function of the oxide thickness before the kinetic transition – comparison with various rate laws.

Fig.13: Schematic description of the oxidation mechanisms in pre- (a) and post-transition (b) stages.

J. Nuclear Materials, 003, 117(2-3), 130-44, doi:10.1016/S0022-3115(02)01704-X

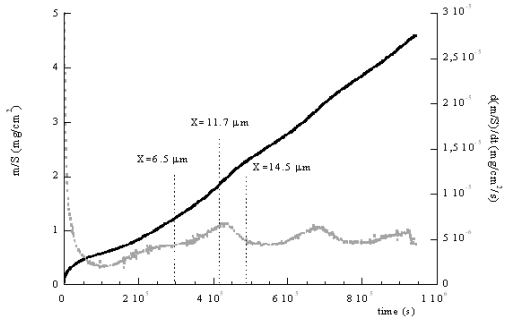

Figure 1

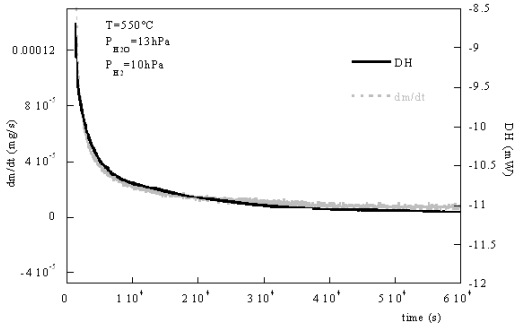

a

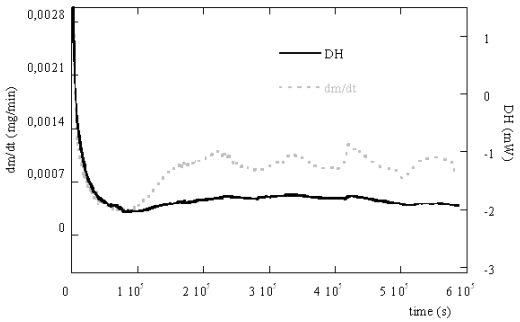

b

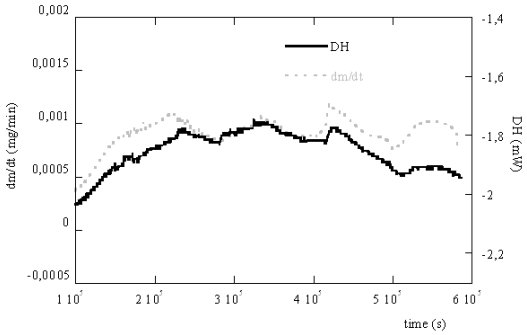

c

Figure 2

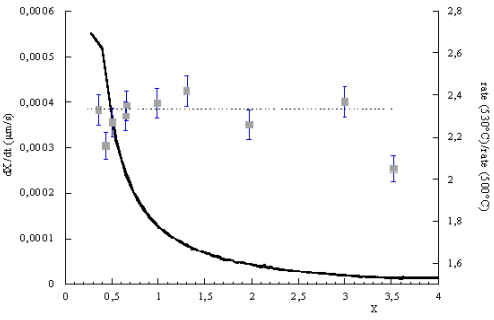

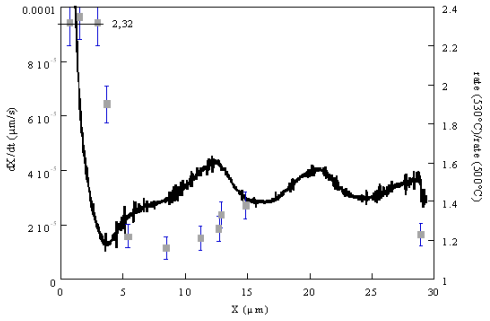

Figure 3

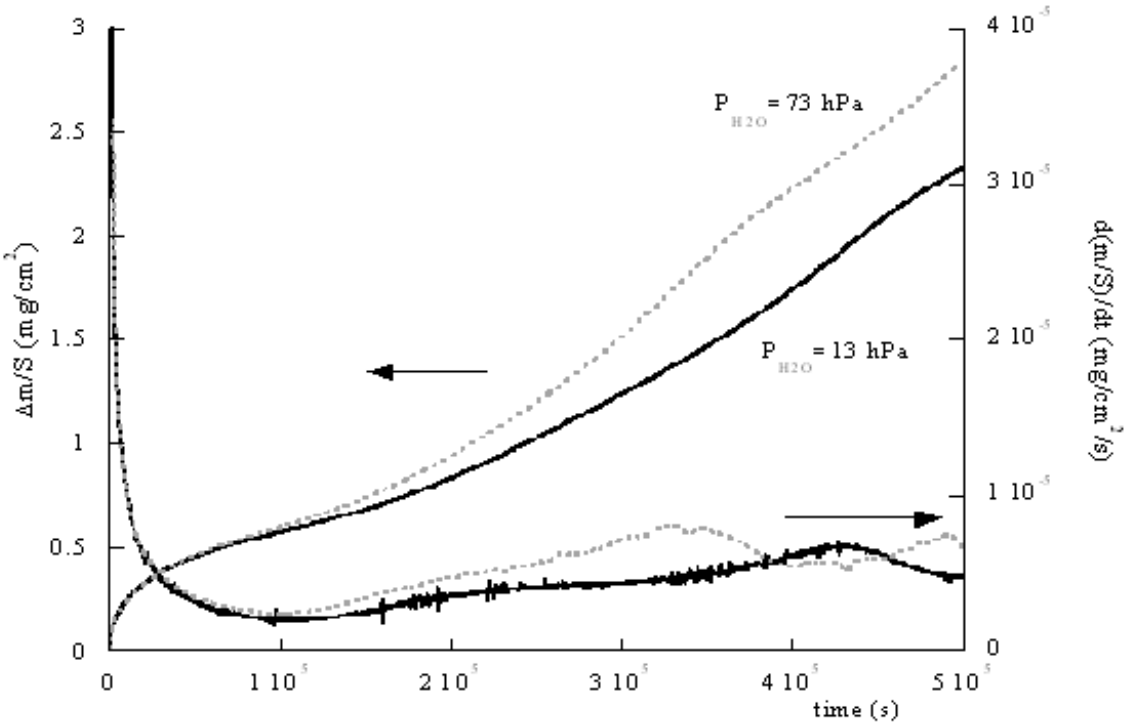

Figure 4

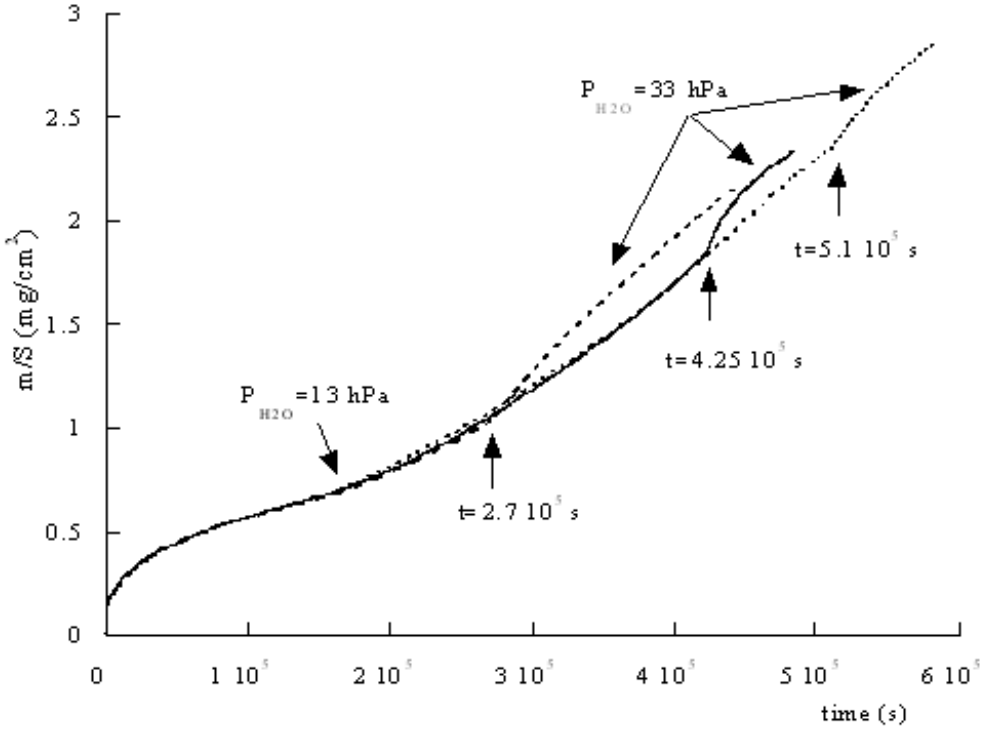

Figure 5

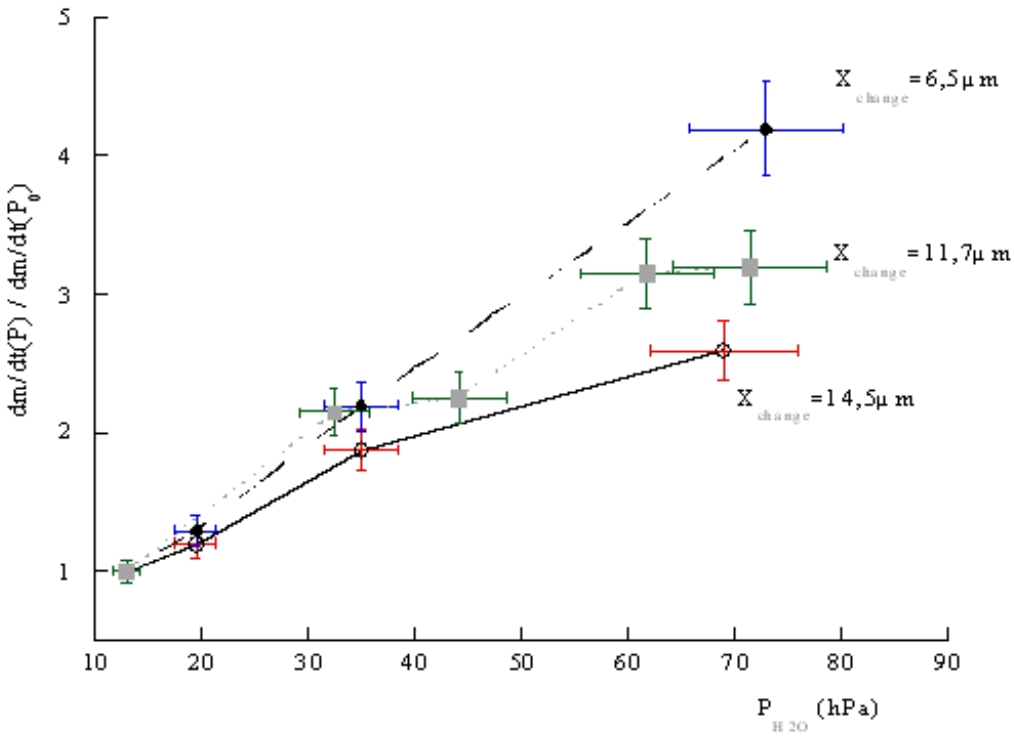

Figure 6

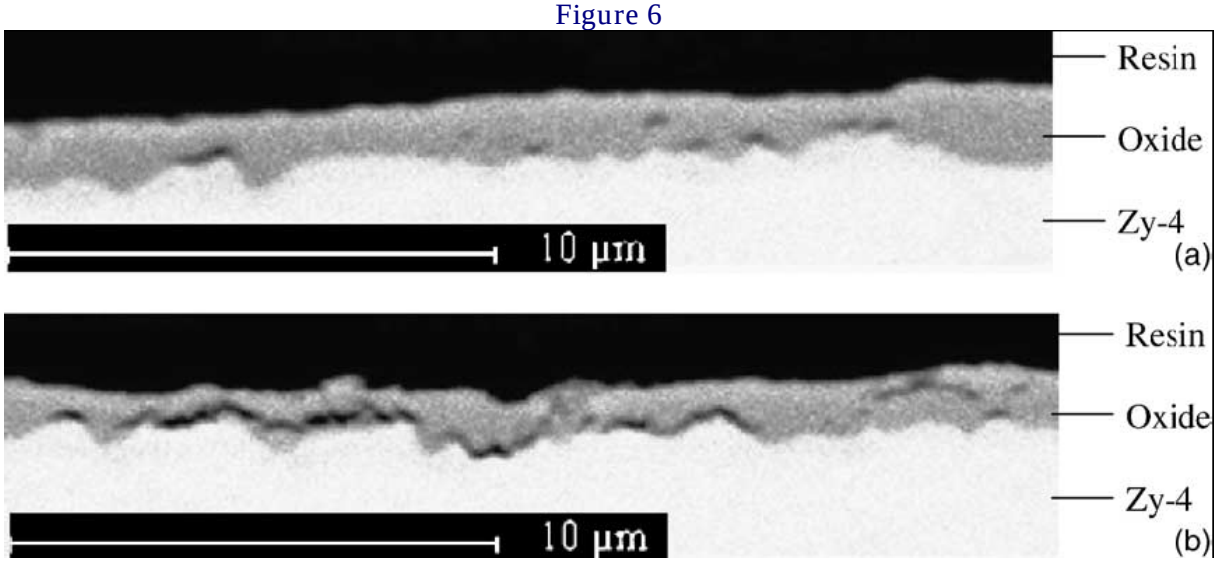

Figure 7

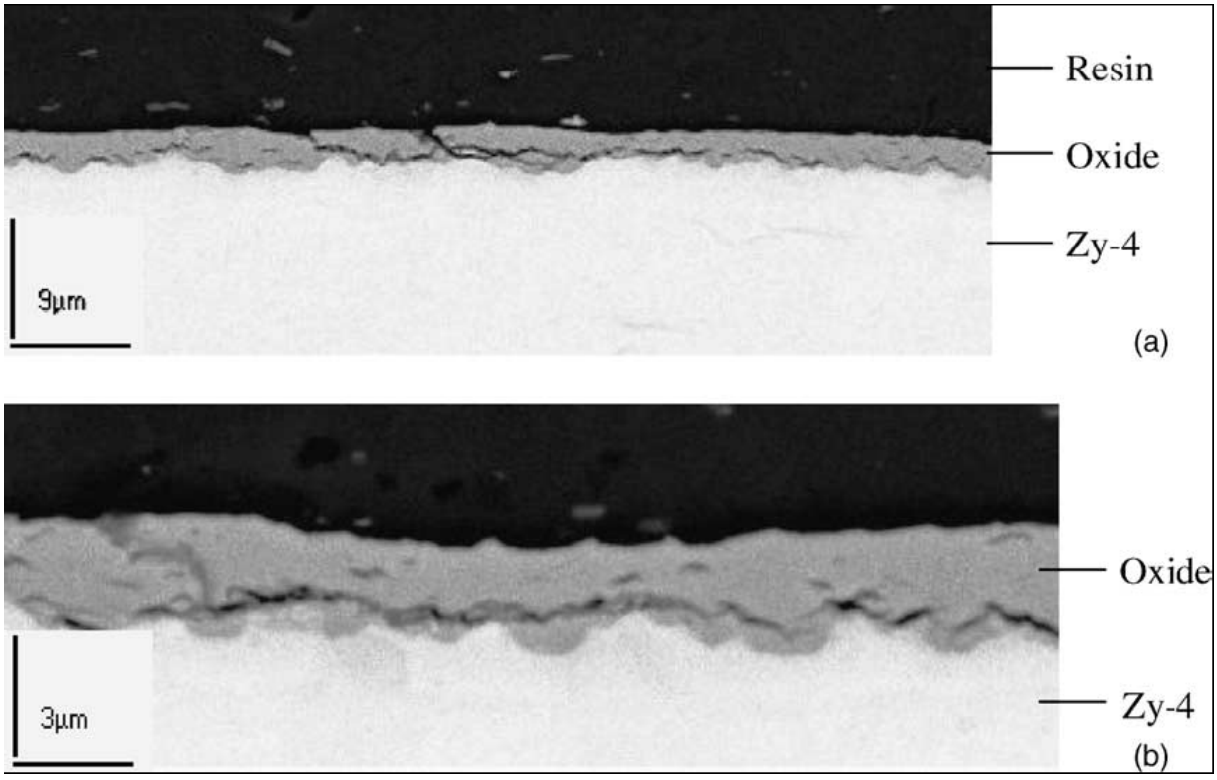

Figure 8

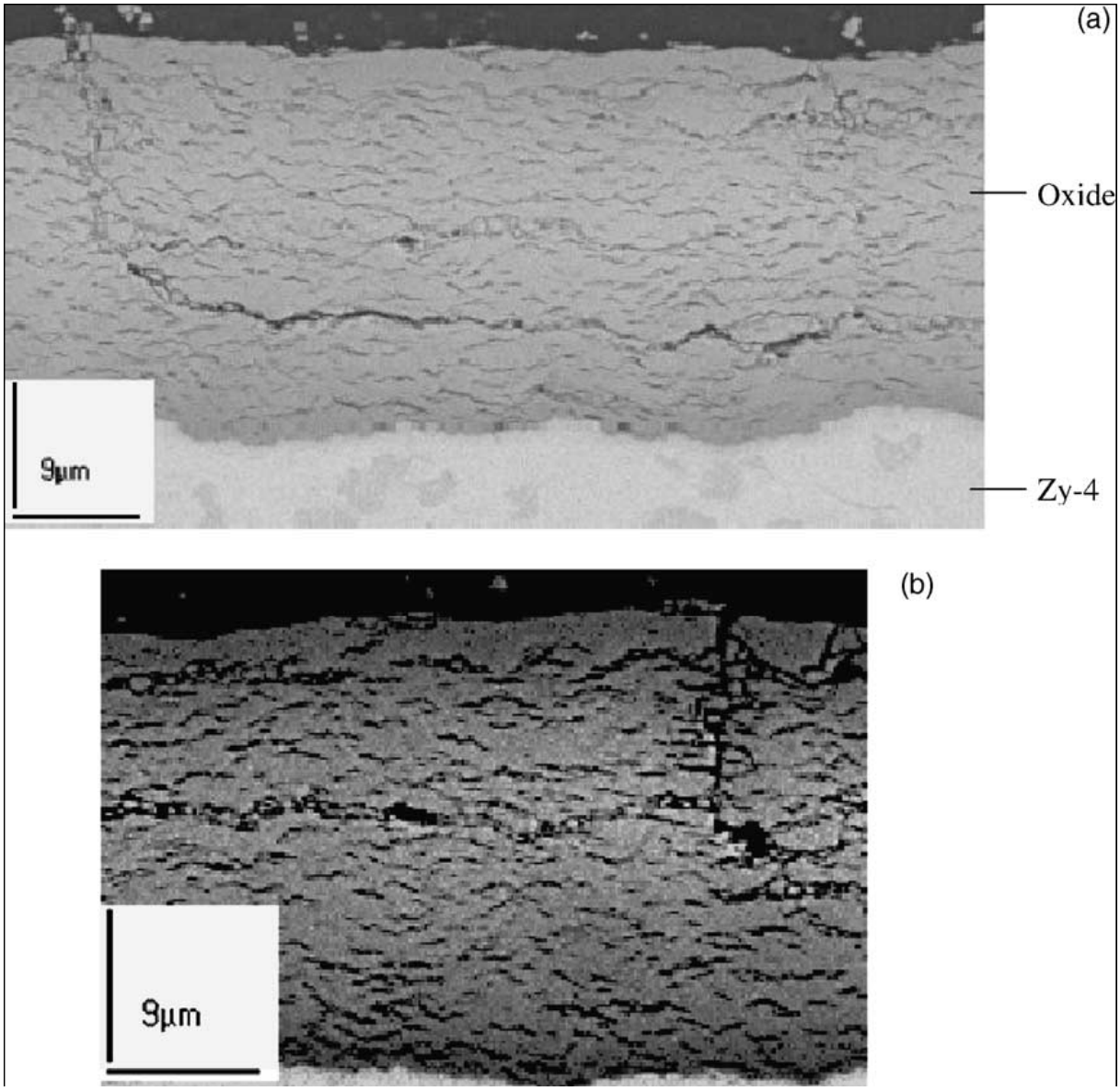

Figure 9

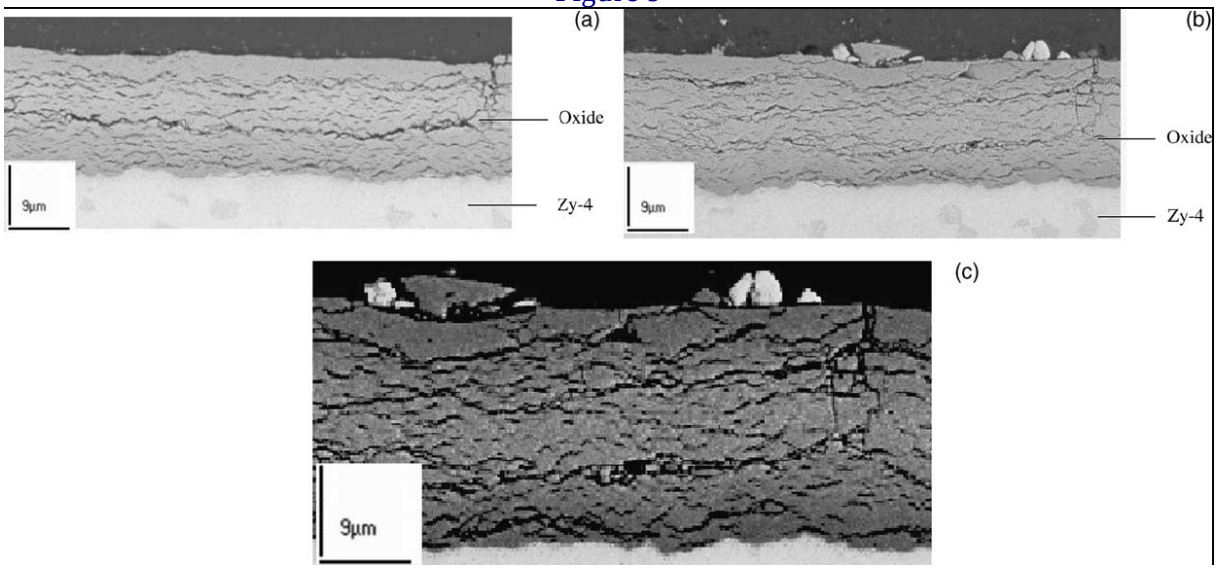

Figure 10

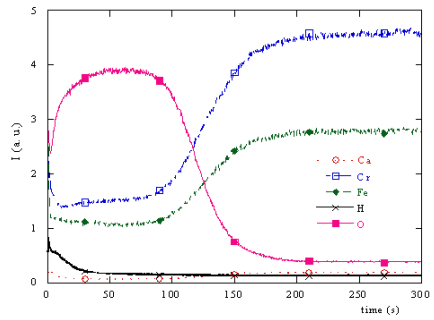

a

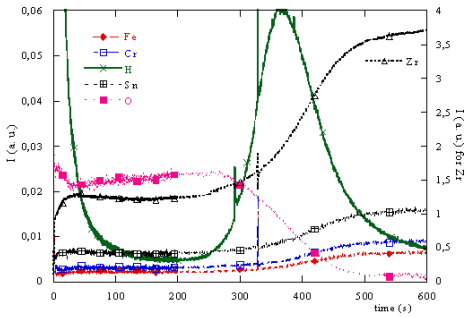

b

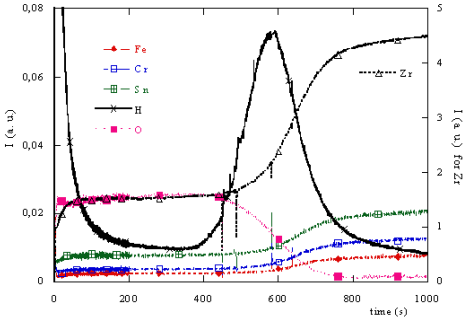

c

Figure 11

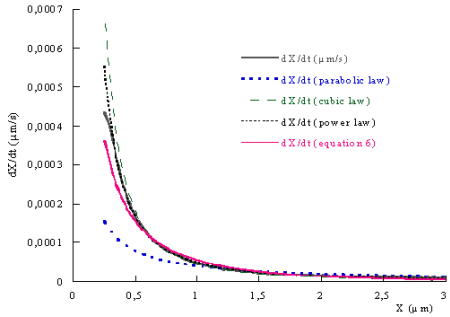

Figure 12

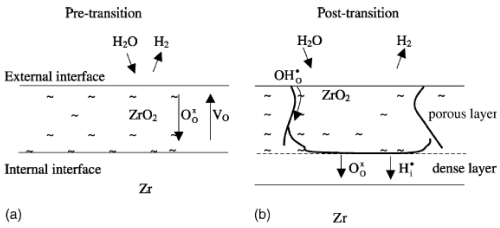

Figure 13